Mass. Inst. of Technology
Cambridge, Mass.

50 pages

Semi-Annual Status Report #1
NASA Grant NAG 5-495

Coordinated Observations of
X-Ray Bright BL Lacertae Objects

C. Megan Urry, Principal Investigator
15 March 1985 - 15 September 1985

This is a semi-annual status report to the National Aeronautics and Space Administration (NASA) concerning NASA grant NAG 5-495. This grant was awarded to Dr. C. Megan Urry of the Massachusetts Institute of Technology in response to a proposal, entitled Coordinated Observations of X-Ray Bright BL Lacertae Objects, to use the International Ultraviolet Explorer (IUE) satellite. The grant was awarded on 3/15/85; this report covers the first six months of its duration, or March 15, 1985 through September 15, 1985.

In April 1985, I had an IUE observing run at the Goddard Space Flight Center (GSFC) in Greenbelt, Maryland. Two BL Lac objects, Mrk 180 and Mrk 501, were successfully observed during two IUE shifts. Concurrently with the observing run, these and several other IUE images of BL Lac objects were analyzed at the IUE Regional Data Analysis Facility (RDAF), which is also at GSFC. The duration of the stay was approximately one week. Funds from grant NAG 5-495 supported this travel. This was the only expenditure during the period March 15 to September 1985 as no observing runs were scheduled in the remainder of 1985.

In the same time period, my co-investigators and I worked on a paper with Japanese collaborators involving IUE observations of the BL Lacertae object Mrk 421. This paper has now been submitted to the Astrophysical Journal, and a copy of the preprint is attached to this report. We anticipate that the observations of Mrk 180 and Mrk 501, also undertaken as part of collaborative broad-band spectral programs, will soon be incorporated into additional publications.

We have been working with several other IUE users and the staff of the RDAF to develop a new program for analyzing IUE spectral images. This method, which extracts spectra from IUE images based on Gaussian fits to spectral crosscuts, will be described in a future report, after the software development is completed.

This concludes the first semi-annual report. Total direct expenditures for the grant were approximately $500 dollars.

Urry

Simultaneous Multifrequency Observations of the BL Lac Object Markarian421

F.Makino[1], Y.Tanaka[1], M.Matsuoka[1], K.Koyama[1], H.Inoue[1], K.Makishima[1], R.Hoshi[2], S.Hayakawa[3], Y.Kondo[4], C.M.Urry[5], S.L.Mufson[6], K.R.Hackney[7], R.L.Hackney[7], S.Kikuchi[8], Y.Mikami[8], W.Z.Wisniewski[9], N.Hiromoto[10], M.Nishida[11], J.Burnell[12], P.Brand[12], P.M.Williams[13], M.G.Smith[13], F.Takahara[14], M.Inoue[14], M.Tsuboi[15], H.Tabara[16], T.Kato[16], M.F.Aller[17], and H.D.Aller[17]

submitted to the ASTROPHYSICAL JOURNAL, Part 1

1986 January

1) Institute of Space and Astronautical Science, Tokyo
2) Department of Physics, Rikkyo University
3) Department of Astrophysics, Nagoya University
4) NASA/Goddard Space Flight Center
5) Center for Space Research, Massachusetts Institute of Technology
6) Astronomy Department, Indiana University
7) Department of Physics and Astronomy, Western Kentucky University
8) Tokyo Astronomical Observatory, University of Tokyo
9) Lunar and Planetary Laboratory, University of Arizona
10) Radio Research Laboratory, Tokyo
11) Department of Physics, Kyoto University
12) Astronomy Department, University of Edinburgh
13) Royal Observatory Edinburgh
14) Nobeyama Radio Observatory*), University of Tokyo
15) Department of Astronomy, University of Tokyo
16) Faculty of Education, Utsunomiya University
17) Radio Astronomy Observatory, University of Michigan

*) NRO, a branch of the Tokyo Astronomical Observatory, University of Tokyo, is a cosmic radio observing facility open for outside users.

ABSTRACT

Simultaneous multifrequency observations of the BL Lac object Mkn421 covering radio through X-ray wavelengths were performed on two occasions separated by five weeks in 1984 January and March, and each observation was coordinated for about a week. We obtained composite multifrequency spectra of the central nonthermal component at the two epochs after subtracting the optical and infrared light of the underlying galaxy. The spectra show the gradual steepening toward high frequency; the power law indices are roughly $\sim$0.1, $\sim$0.6, and $\sim$1.0 for radio, infrared-optical and UV bands, respectively. The UV and optical-infrared fluxes decreased by about 20 percent in five weeks, while the radio flux remained stable. The X-ray flux decreased by a factor of $\sim$2 and the change was more pronounced at hard X-rays, which suggests that X-ray emission possibly consists of two components. The degree of polarization at the optical band varied on the time scale of a few days while the position angle remained unchanged.

Physical parameters of Mkn421 are discussed in terms of the synchrotron self-Compton model. Taking the spectral turnover between infrared and radio for synchrotron self absorption, the radio emission originates in a more extended region than the infrared to X-ray emission, the source size of which should be less than about 10^{-2} milliarcseconds. Relativistic beaming is required if the angular size is smaller than a few times 10^{-3} milliarcseconds. A possible explanation of the spectral change during the two epochs is also discussed.

Subject headings: BL Lacertae objects - radiation mechanisms -
polarization - X-rays:Sources

I. INTRODUCTION

The central problem of active galactic nuclei (AGN) is the emission mechanism of the continuum radiation at radio through gamma-ray frequencies, and the ultimate energy source of that radiation. Apparently these AGN somehow generate very high luminosities (assuming cosmological distances and isotropic emission) inside very small volumes (as deduced from variability timescales). BL Lac objects are distinguished from other classes of AGN by their rapid variability, high degree of polarization, and general lack of discrete spectral features. These properties are useful diagnostics of the radiation processes. Simplified models such as the synchrotron self-Compton model with or without relativistic beaming have been proposed to explain many of the observed characteristics of BL Lac objects and other AGN. A high degree of polarization in the infrared and optical region may be evidence of a synchrotron process, a hypothesis that can be strengthened if correlated temporal changes in radio, infrared, and optical bands are detected. Many AGN have been observed simultaneously in various frequency bands from radio to X-ray frequencies in order to search for correlated variations within an individual spectrum (Kondo et al. 1981; Bregman et al. 1982, 1984; Worrall et al. 1982, 1984a, 1984b, 1984c; Wills et al. 1983; Mufson et al. 1984; Glassgold et al. 1983; Hutter and Mufson 1985). The absence of discrete spectral features, often a nuisance when determining the physical state of the emitting region, in this case provides a conveniently uncontaminated broad band spectrum.

Mkn421 was first noted as a blue excess object which turned out to be an elliptical galaxy with a bright, point-like nucleus. The redshift of the galaxy was measured to be z=0.03 (Ulrich et al. 1975) but the spectrum of the nucleus was featureless. It also showed the optical polarization and flat radio spectrum, common to BL Lac objects (Maza et al. 1978; O'Dell et al. 1978a). The angular size of the radio source associated with Mkn421 is less than 1 milliarcsecond (mas) at 6cm (Weiler and Johnston 1980; Baath et al. 1981). The ultraviolet emission from Mkn421 has been monitored over the past seven years with the International Ultraviolet Explorer (IUE) satellite. Nine IUE spectra obtained between 1978 and 1981 showed some variability, but no or only very weak correlation between flux level and spectral index (Ulrich et al. 1984). Since it is one of the brightest BL Lac objects known in the X-ray band, Mkn421 has been observed fairly often with various X-ray instruments (see summary of observations and references in Urry et al. 1985). X-ray observation of Mkn421 with HEAO-1 satellite detected a change in spectral index from 2.1 to 3.9 and the disappearance of the hard component above 10keV by comparing with earlier observations with OSO-8 and SAS-3 satellites (Mushotzky et al. 1979). Because of the lack of simultaneity among the observations at radio through X-ray frequencies, correlations among intensity changes have been poorly studied.

We made simultaneous multifrequency observations of the BL Lac object Mkn421 at radio, infrared, optical, ultraviolet, and X-ray frequencies on two occasions in 1984 January and March. In § II we summarize observations performed at each frequency band and we describe the composite spectrum thus obtained at each of the two epochs. In § III

interrelations among various observed bands and the comparisons with previous observations are discussed. In § IV an interpretation of those results in terms of the synchrotron self-Compton model is attempted. Conclusions will follow in § V.

II. OBSERVATIONS

The observation was conducted at the radio, infrared, optical, ultraviolet and X-ray bands on two occasions separated by five weeks, 1984 January and March. The coverage of the observed frequency bands and the instruments utilized in the present observations are summarized in Table 1.

Table 1

a) X-ray observations

X-rays were observed with two sets of the scintillation proportional counters (SPC-A and SPC-B) on board the TENMA satellite (Tanaka et al. 1984; Koyama et al. 1984). The observed energy range was 1.5 to 35keV, but above about 10keV, the flux was too faint to discriminate from the background. The day-to-day variations of the integrated energy flux over the energy range 1.5-10keV are depicted in the lowest panel of Figure 1. The statistical accuracy of day-to-day

data was not good enough to obtain the energy spectrum. Then we summed up the data for each observation period; the time-averaged energy spectra observed in January and March are shown in Figure 2.

Figures 1 and 2

The flux decreased by a factor of about two from January to March. Particular attention has been paid to the spectral analysis, since for faint sources such as Mkn421 the spectral shapes depend critically on background subtraction. The properties of the background spectrum have long been studied carefully using extensive data sets compiled from TENMA (Koyama et al. 1984). Before summing the data from SPC-A and SPC-B, the spectral analysis was independently carried out for each data to check the consistency of the results. The spectra obtained independently from SPC-A and SPC-B were combined to improve statistics, after confirmation of consistency. The best fit power law index for the January and March observations over 1.5-10keV is 1.1±0.2 and 1.8±0.3 with the normalization factor $(1.01\pm0.17)\times10^{-2}$keV/cm^2 sec keV and $(8.7\pm2.4)\times10^{-3}$keV/cm^2 sec keV at 1keV, respectively.

It is, however, to be noticed that the single power law fit is only marginally acceptable, since the reduced χ^2 value is 2.3 (degree of freedom; 11) and 2.2 (degree of freedom; 7) for the January and March data, respectively. The deviations from the single power law models are evident above 4keV. The spectrum obtained in January is flatter above 4keV as compared to March observations. Below 4keV, on the other hand,

the spectral index is 1.6±0.2 and 1.7±0.3, respectively. While the intensity varied by a factor of two.

We notice that the EXOSAT satellite also observed Mkn421 in the period 1984 February 1 to 6, one week after our January observation (Warwick et al. 1985). The intensity and spectral index are intermediate between those of our January and March observations.

b) UV observations

Ultraviolet observations were made by the short wavelength prime (SWP) and the long wavelength prime (LWP) cameras of the IUE satellite on 5 occasions during the present program. The results are summarized in Table 2. The integrated fluxes are plotted in the fifth panel of Figure 1. The spectra were extracted from the line-by-line file using a customized narrow slit to maximize the signal-to-noise. Data points contaminated by reseaux or cosmic ray hits were removed, and the data were then binned in intervals of approximately 25Å. The binned data points were weighted according to the rms deviations within the bins and were fit to a power law spectrum using a least-squares procedure for 1200-3000Å range.

Table 2

It is to be noted that the integrated ultraviolet flux decreased by 20∿30 percent from January to March and the spectral index α shows a

slight steepening (a change of α roughly 0.1).

c) Optical observations

Optical observations were made at the Okayama Astrophysical Observatory, the Dodaira Station, and the Mt. Lemon Observatory. Five telescopes were used with various diaphragm sizes, which are listed in Table 3.

Table 3

Mkn421 is found at the core of a giant elliptical galaxy and, in particular, optical and infrared fluxes are contaminated by galaxy emission. Therefore, we must subtract the galaxy component to obtain the flux from the central compact core. The distribution of the surface brightness of the galaxy was studied by Kinman (1978), Mufson et al. (1980), and Hickson et al. (1982) but some discrepancies remained among their results. Kikuchi and Mikami (1986) also made the multi-aperture photometry of Mkn421 and obtained a result similar to that by Kinman (1978). In the present study, the subtraction of the contribution from the underlying galaxy has been made using the results by Kikuchi and Mikami (1986). The corrections for the apertures used in the observations are also tabulated in Table 3. The colors of the underlying galaxy are taken to be constant as U-B=0.46, B-V=1.05 and V-R=0.90 after Kikuchi and Mikami(1985). These colors are consistent with those of a

redshifted elliptical galaxy at z=0.03. For R-I, the mean value of 0.78 for elliptical galaxies (Johnson 1966) is assumed, since the measurement of the underlying galaxy has yet to be made at the I band.

The observed fluxes and the fluxes of the nonthermal component are tabulated in Table 4. The day-to-day variation of the flux of the nonthermal component at the V band is shown in the fourth panel of Figure 1. The nominal errors associated with the observed fluxes are typically 2~3 percent but 1 percent for several cases at Dodaira in March. However, the derived flux of the nonthermal component shows a scatter greater than the observational errors reaching about 10 percent, depending on the aperture and/or telescope. A part of this scatter is certainly caused by the incompleteness of the subtraction of the galaxy contribution. Although we have no reasonable explanation for the remaining scatter, we suspect that the seeing condition and the scattered light of a nearby 6 mag star affect the measurement of the extended source and of the sky brightness, respectively.

Table 4

Continuum spectra for both observing periods are shown in Figure 3 as well as those in the infrared region. In the January data of the fluxes in the B and V bands, we find a systematic difference between the data obtained by the 100cm telescope at Mt. Lemon and those by the 188cm telescope at Okayama, although the spectral indices coincided well with each other. The difference amounts to 7 percent, and the origin of the

difference is unknown. For the spectra in the March epoch, we used the results after March 4, since the optical flux abruptly decreased around March 3 but stable thereafter.

Figure 3

The average V band intensities in January and March were 8.9±0.5mJy and 7.8±0.5mJy, respectively. The spectral index in the UVBR region varied from 0.65±0.15 to 0.76±0.10 from January to March. Slight darkening and spectral steepening are barely significant, if we consider only the data in the optical region. It should be also noted that, in early February, a brightnening to 10.4±0.3mJy in the V band with a spectral index of 0.72±0.06 has been observed at Dodaira.

Optical polarimetry was also made simultaneously with the photometry by the 188cm telescope at Okayama, and by the 91cm telescope at Dodaira. The polarization of the nonthermal component showed no wavelength dependence in the UBVR region throughout the whole observing period, provided that the light from the underlying galaxy was unpolarized. The polarization properties of the nonthermal component through the U to K bands averaged over March 8-12 are given in Table 5. No wavelength dependence of the degree of polarization was found in the optical and near infrared regions.

Table 5

The variation of the degree of the polarization is shown in the first panel of Figure 1. The degree of polarization showed a considerable change during the March epoch; from February 29 to March 5 the degree of polarization was as high as 7∿8.5% with a trend of the smooth weakening and on March 6 it declined abruptly to 4∿5%, while the position angle remained constant at 170∿180 degrees. This abrupt change of the polarization seems to be correlated with the flux decrease in the same period.

d) Infrared observations

Infrared observations were made with the 3.8m telescope at United Kingdom Infrared Telescope (UKIRT) at Mauna Kea, Hawaii and the 1m telescope at the Agematsu Infrared Observatory. At Agematsu we observed Mkn421 on January 25 and 27 and March 7 and 8 with a rectangular aperture of 24" in the right ascension by 60" in the declination and 40" chopping throw at the J, H and K bands. The calibration was made by using ξUMa as a standard star and SA0062387 as a reference star. UKIRT observations were made on February 4 and 6 at the J, H, K and L bands with a 18" aperture using GL299 as a reference star. On March 8-12, the J, H, K and L' bands observations were made with 4.8", 7.8" and 11.8" apertures, on March 11-12 the M band observation with a 4.8" aperture, and on March 8-10 the N band observation with a 6" aperture. On January 30, photometry at J, H, K, and L bands was made with a 8" aperture using the NASA infrared telescope, at Mauna Kea, Hawaii.

The observed data are tabulated in Table 6. The infrared flux decreased by 13±4 percent from January to March comparing the Agematsu observations at two epochs. As in the optical observations, the contribution of the underlying galaxy was subtracted to obtain the fluxes of the central nonthermal component for J, H, K, L (L') bands. Since the observation with the largest beam size of 24"×60" does not agree with the brightness of the model galaxy, we obtain contrariwise the brightness of the underlying galaxy for the 24"×60" beam size by subtracting the nonthermal component derived from the observations with smaller beam sizes on March 8, and apply it to the photometry in the January epoch. The infrared colors of the undelying galaxy are obtained as J-H=0.69 and H-K=0.40 from the observations in March, which become almost consistent with those of typical elliptical galaxies (Frogel et al. 1975; Persson et al. 1979; Glass 1984) taking account of the K-corrections (Frogel et al. 1978). We assumed K-L=0.06 (Aaronson 1978) and V-K=3.40 (Aaronson 1978; Persson et al 1979), consistent with those of typical elliptical galaxies including K-corrections. For the M and N bands the contribution of the galaxy is safely neglected. The resulting fluxes of the nonthermal component are summarized in the bottom panel of Table 6 and the flux at the K band is plotted in the third panel of Figure 1. The spectra obtained for respective epoch are shown in Figure 3 along with the optical spectra. The spectral index in the infrared band was 0.5±0.2 and 0.57±0.11 for January and March, respectively. The conversion of the magnitude to the absolute flux has been made using coefficients tabulated in Table 6, on the basis of the calibration by Blackwell et al. (1983).

Table 6

The polarization measurements were also made on March 9, 11 and 12 at the J, H and K bands by UKIRT. Those results are tabulated in Table 5 together with the optical polarization. The degree of polarization and the position angle of the nonthermal component in the infrared are 4.8±0.4 percent and 180±5 degrees, which are fully consistent with those at optical bands.

e) Radio observations

Radio observations were made with the 45m telescope at the Nobeyama Radio Observatory and the 26m telescope at the University of Michigan. At Nobeyama, flux measurements at 10, 22 and 43GHz were made, while at Michigan flux was measured at 4.8, 8.0 and 14.5GHz. At Nobeyama the calibration was done by using 3C286 as the primary calibrator of which fluxes are 4.7, 2.6 and 1.7Jy at 10, 22 and 43GHz, respectively, and 3C274, 4C39.25 and 1144+40 were observed as references. No significant daily variations above 10 percent level were found, so that only the averaged data over each epoch are used. The results are listed in Table 7, from which one sees that radio fluxes are rather stable and 560, 520 and 480mJy at 10, 22 and 43GHz, respectively, throughout January and March observations.

Table 7

The data obtained at Michigan are consistent with those at Nobeyama, 670, 610 and 550mJy at 4.8, 8.0 and 14.5GHz, respectively. In the second panel of Figure 1, the data at 14.5GHz are plotted.

f) Composite spectra

Figure 4 shows the composite energy spectra emerging from the central nonthermal component of Mkn421 in 1984 January and March. These composite spectra are similar to those of other BL Lac objects, i.e., a power law spectrum with a gradually increasing spectral index toward high frequencies. In the January epoch, the spectral indices are $\sim$0.1, $\sim$0.5, $\sim$0.7, $\sim$1.0 and $\sim$1.1 for radio, IR, optical, UV and X-ray wavelengths, respectively, while in March these are $\sim$0.1, $\sim$0.6, $\sim$0.8, $\sim$1.1 and $\sim$1.8.

Figure 4

III. COMPARISON WITH PREVIOUS OBSERVATIONS

At radio wavelengths, VLBI observations (Baath et al. 1981; Baath 1984) revealed an unresolved core of 240±40mJy with a size less than

0.3mas as well as a resolved component of 270±50mJy and 3.4mas size at 5GHz. Other VLBI observations (Weiler and Johnston 1980; Wehrle et al. 1984) also revealed a compact component of ∿1mas size and ∿300mJy strength both at 5GHz and 2.3GHz. There also exists a ∿0.1Jy extended component of a few arcmin size (Kapahi 1979; Ulvestad, Johnston and Weiler 1983). Our flux measurements at radio frequencies included all these components. But the total flux of Mkn421 was rather stable at centimeter wavelength and our value is consistent with previously reported values (Margon, Jones, and Wardle 1978; O'Dell et al. 1978a). Therefore the flux of the core component is probably about 300 mJy.

O'Dell et al. (1978a) showed that the radio spectrum extends to at least 90GHz with a flat shape. The extrapolation of the flat radio spectrum of 300mJy intersects the extrapolation of the IR-optical spectrum at around 10^{12}Hz.

The optical fluxes were faint compared to the previous observations (Hagen-Thorn et al. 1983). Also the infrared fluxes of the nonthermal component were in a faint phase among previous observations at the K band (Ulrich et al 1975; Allen 1976; Joyce and Simon 1976; O'Dell et al. 1978b; Baily et al. 1981; Impey 1983). Thus we conclude that Mkn421 was in a dark phase on two occasions of our coordinated observations.

The position angle of the optical polarization in the present observation agrees with the dominant direction in the long term behavior (Hagen-Thorn et al. 1983). The polarization of Mkn421 observed by Baily et al. (1981) in 1980 December is nearly equal to that in the present observation in the position angle and the degree of polarization, though Mkn421 was in a brighter phase then. However Bailey et al. claimed that the polarization degree decreases as the wavelength increaces, while our

degree of polarization shows no wavelength dependence. We think it is not due to observational errors but due to the difference in the models of the underlying galaxy. Their model galaxy has the brightness by 0.3mag smaller than that we used in the V band, which brings a decreasing degree of polarization as the wavelength increases through the dilution effect. Therefore, a decreasing polarization of Mkn421 with wavelength is questionable.

It is to be noted that there exists a spectral break between IR-optical and UV bands at around 10^{15}Hz. This spectral break or steepening seems to be common to BL Lac objects.

The UV light curve for the period 1978-1981 was analyzed by Ulrich et al. (1984), and they have shown that the flux varied on the time scale of a few years. In 1979 November the UV flux was in a minimum state with the spectral index of 1.0. Both the flux and the spectral index are similar to those of the present observation in 1984. Since the flux steadily increased and the spectrum hardened from 1979 to 1981, Mkn421 might have turned to a decreasing and softening phase in 1982-1983.

The X-ray flux of this observation is significantly lower than those of previous observations by SAS 3 (Hearn et al. 1979) and HEAO 1 (Mushotzky et al. 1979) by an order of magnitude. At those epochs X-ray fluxes were higher than or on the extrapolation from the UV spectrum. The extrapolation of the UV spectrum toward shorter wavelengths should be compared to the X-ray spectra obtained by TENMA. The extrapolation from the UV spectrum lies at 5.47 and 2.26μJy at 10^{18}Hz at January and March epochs, respectively, while the observed fluxes were 1.1 and 0.51μJy, respectively. Then the observed X-ray fluxes are lower than the

extrapolation from the UV spectrum by an order of magnitude in the present observation. The spectral slope between UV and X-ray is 1.3∿1.4 and apparently steeper than the UV slope of ∿1. On the other hand, the X-ray spectral index changes from ∿1 at the January epoch to ∿2 at the March epoch. Below 4keV the X-ray spectral index was about 1.5 for both periods.

This result implies that X-ray emission is represented by two components. These variations of flux and spectral shape at five week interval are very important feature. HEAO-1 observations in 1978 May showed a remarkable spectral change from OSO-8 observations in 1977 May (Mushotzky et al 1979). It has been suggested that the X-ray spectra of BL Lac objects have two components, a soft and a hard component (Riegler et al. 1979; Worrall et al. 1981). We may infer that the hard component varies more violently than the soft component.

IV. IMPLICATIONS ON THE MODEL

a) Source parameters

The continuum emission from BL Lac objects may be due to synchrotron radiation and/or inverse Compton scattering (Blandford 1984; Konigl 1981). In this subsection we derive physical parameters of the source using the data obtained in the present observations within the context of the homogeneous and spherical symmetric synchrotron self-Compton (SSC) model (Gould 1979). The SSC model assumes the presence of relativistic electrons with power law distribution, $N(\gamma) \propto \gamma^{-p}$

(Υ is the Lorentz factor and p is the power law index), which emit synchrotron radiation having the power law spectrum $S_{syn} \propto \nu^{(1-p)/2}$. Since the synchrotron absorption coefficient is proportional to $\nu^{-(4+p)/2}$, the self absorption turnover is expected at a certain frequency ν_a (ν_*GHz) with the corresponding flux density S_*Jy.

Common to those BL Lac objects for which the optical and UV fluxes were observed, a break or bending of the spectrum appears at the break frequency $\nu_b \sim 10^{15}$Hz. The acceleration rate of relativistic electrons responsible for synchrotron radiation above ν_b may be smaller than the energy loss rate, making the energy spectrum steeper. Here the Lorentz factors of electrons which emit the synchrotron radiation at the turnover and break frequencies are denoted by Υ_a and Υ_b, respectively. Soft x-rays in January epoch and the whole X-ray in March epoch may be produced by the synchrotron radiation by electrons in the high energy tail. The relatively flat hard X-ray component as seen in the January spectrum (see Figure 2) may be attributed to the self-Compton photons, i.e., inverse Compton scattering of synchrotron photons off relativistic electrons. This self-Compton flux S_{com} has a power law spectrum with the same spectral index as the synchrotron spectrum with

$$S_{com} \propto \nu_X^{-(p-1)/2} \theta_*^{-2(p+2)} \nu_*^{-(3p+7)/2} S_*^{(p+3)} (\delta/(1+z))^{-(p+3)} \ln(\nu_b/\nu_a), \quad (1)$$

where ν_X is the frequency of a scattered photon, δ is the kinematical Doppler factor in the relativistic beaming model, z is the cosmological redshift, and the apparent angular diameter of the source is θ_*mas.

Eenergy densities of magnetic fields u_{mag} and synchrotron photons u_{syn}, the lower limit to the energy density of relativistic electrons

u_{rel}^{min}, and γ_a are given as

$$u_{mag} \propto \theta_*^{8} \nu_*^{10} S_*^{-4} (\delta/(1+z))^2, \tag{2}$$

$$u_{syn} \propto \theta_*^{-2} \nu_* S_* (\delta/(1+z))^{-4}, \tag{3}$$

$$u_{rel}^{min} \propto \theta_*^{-9} \nu_*^{-7} S_*^{4} (\delta/(1+z))^{-5} (1+z)^2 d_{L*}^{-1}, \tag{4}$$

and

$$\gamma_a \propto \theta_*^{-2} \nu_*^{-2} S_* (\delta/(1+z))^{-1}, \tag{5}$$

respectively (Marscher et al. 1979; Marscher 1983). Here d_{L*}Gpc is the luminosity distance. The proportional coefficients in Equations (1)~(5) are complicated functions of p.

Since the X-ray flux by the self-Compton photons should be lower than the observed X-ray flux, we obtain the lower limit to the beaming factor δ_{min} from Equation (1) as,

$$\delta_{min} \propto (1+z) S_* \left(\frac{\ln(\nu_b/\nu_a)}{\nu_X^{(p-1)/2} \theta_*^{2(p+2)} \nu_*^{(3p+7)/2} S_*} \right)^{1/(p+3)} \tag{6}$$

The synchrotron self absorption turnover was not directly observed, but presumably ν_* lies at around $\sim 10^3$, the intersection of extrapolations from radio and IR spectra. Assuming that the flux at the turnover is not much different from that of the smallest unresolved radio component (0.3Jy with an angular size less than 0.3mas), we adopt S_*=0.3. The turnover frequency ν_* is determined so that the synchrotron

flux gives the observed UV flux at 10^{15}Hz (6.5mJy for the January epoch and 5.1mJy for the March epoch) with the spectral index α=0.625 (p=2.25) the well fitted value to the IR-optical observations. The source parameters are calculated as a function of θ_*, which are shown in Figure 5 for the January data. We notice that there are two critical values of θ_*, referred to as θ_1 and θ_2. For $\theta_*>\theta_1$, γ_a is less than unity. Since the synchrotron flux with a power law spectrum is valid for $\gamma>>1$, thus, θ_1 provides an optimistic upper limit to the angular diameter. While for $\theta_*<\theta_2$, the expected inverse Compton flux at ν_X deduced from the observed synchrotron flux exceeds the observed flux if δ=1, i.e., no reletivistic bulk motion of the source is invoked. Conversely such relativistic effects are required if θ_* is found virtually smaller than θ_2. In the first and second columns of Table 8, the results for the January and March data are tabulated for δ=1 and $\theta_*=\theta_2$, taking $\nu_X=10^{18}$Hz.

Figure 5 and Table 8

Ulrich et al. (1975) reported the absorption redshift of the underlying galaxy, z=0.03, implying the distance of $90h^{-1}$Mpc; 1mas corresponds to $0.44h^{-1}$pc and the light crossing time of the source is $t_{1c}=4.5\times10^{7}\theta_* h^{-1}$sec, where h is the Hubble parameter in units of 100 km s^{-1} Mpc^{-1}. In Table 8 the cooling times, t_a and t_b, of electrons with Lorentz factors of γ_a and γ_b, are given respectively, as well as t_{1c}. The cooling time of electrons responsible for the IR-optical radiation is shorter than the light crossing time, implying in situ acceleration

of the relativistic electrons. Also from Table 8 one sees that the energy density of magnetic fields, u_{mag}, dominates over that of relativistic electrons, noting that u_{rel}^{min} is not so different from true energy density of relativistic electrons since γ_a is relatively small. This property is consistent with the observed behavior of polarization in the IR-optical bands that the position angle remained constant although the degree of polarization and flux varied with time.

Since VLBI experiments have shown that ∿1mas structure exists at 5GHz, radio structure should be more extended than IR-optical-UV component. This is consistent with the model of flat spectrum radio sources which can be expressed in terms of inhomogeneous synchrotron source (Marscher 1977; Konigl 1981). In this model the apparent angular size is inversely proportional to the frequency in the flat portion of the spectrum, and the size at 10^{12}Hz becomes $\sim 5\times10^{-3}$mas, consistent with above analysis.

Mkn421 was rather faint in the epoch of the present observation and the total luminosity was about 10^{44} erg s^{-1}. At the most luminous epoch in the past it was about 10 times brighter. If we adopt that the ultimate energy release occurs as a result of accretion onto the supermassive black hole and 10^{45} erg s^{-1} corresponds to the Eddington luminosity, the mass of the black hole is $10^7 M_\odot$ and the accretion energy is reprocessed in the size of 10^{13}cm which amounts to $\theta_* \cong 10^{-5}$. Thus the size of the synchrotron source is about 10^2 times larger than the size of the ultimate energy release region.

(2) Spectral variation

Our January and March observations of Mkn421 suggest that the self-Compton flux corresponding to the relatively flat hard X-ray tail seen in the January observations decreased by more than factor $\sim$2 during five weeks, while the synchrotron flux decreased by 15$\sim$25 percent in the IR, optical and UV bands in the same interval. The radio flux remained essentially constant during those two observational periods. It is , however, rather difficult to explain the change of the spectra obtained in those two epochs with the homogeneous and spherical symmetric SSC model as will be discussed below.

As seen in Equation (2)-(5), the physical source parameters are determined as functions of p, θ_*, S_*, ν_* and δ. Comparing the composite spectra of the two epochs we may approximate that S_* and p remained constant, and that ν_* decreased by 35 percent resulting in a decrease of the synchrotron flux by 22 percent. Let us first consider that ν_* alone decreased, and θ_* and δ remained constant. Physically the decrease of ν_* is a consequence of the decrease of u_{mag} and the increase of u_{rel}^{min}. In this case the self-Compton flux increases by a factor of 14 since $S_{com} \propto \nu_*^{-(3p+7)}$ from Equation (1), on the contrary to the observed spectral change.

Next let us assume that in addition to the decrease in ν_* the source expands as $\theta_* \propto \nu_*^{-\beta}$ where β is an arbitrary constant. From Equations (1) $S_{com} \propto \nu_*^{8.5\beta-6.875}$ for p=2.25. In order to reduce the self-Compton flux at 10^{18}Hz by a factor of 2.2, from 1.1μJy in January to 0.51μJy in March, we have $\beta>1.04$. In this case, however, u_{mag} and u_{rel}^{min} change as $u_{mag} \propto \nu_*^{10-8\beta}$ and $u_{rel}^{min} \propto \nu_*^{9\beta-7}$. As a result, the total magnetic energy increases, since it chages as $\theta_*^3 u_{mag} \propto \nu_*^{10-13\beta}$. Thus, in order to explain the observed spectral variation, the increase in the

magnetic field energy is necessary despite the expansion of the source. In the case of adiabatic expansion, u_{mag} is proportional to θ_*^{-4}, implying $\beta=5/6$, which results in $S_{com} \propto \nu_*^{0.21}$. Therefore, the decrease of the self-Compton flux is less than that of the synchrotron flux in contrast to the observational fact.

Finally, we consider the change of the relativistic beaming factor along with the adiabatic expansion of the source. For $u_{mag} \propto \theta_*^{-4}$, Equation (2) implies $\nu_* 10\delta^2 \propto \theta_*^{-12}$, from which we obtain $S_{com} \propto \nu_*^{(p-1)/6} \delta^{-(2p+7)/3}$. In order to decrease the self-Compton flux by a factor of 2.2, the kinematical Doppler factor is required to increase by 20 percent within five weeks and the source would expand during the above time interval by 34 percent. Accompanying this u_{mag} and u_{rel}^{min} would decrease by a factor of 3.2 and 2.3, respectively. Thus the increase in the relativistic motion of the source can account for the observed property of the spectral variation separated by five weeks, although some acceleration mechanism must be invoked. In the third column of Table 8, the source parameters in the March epoch are shown assuming that the source in January was in a state of $\theta_*=\theta_2$ and $\delta=1$.

Since the hard X-ray spectrum was very steep in March, we obtain more severe limit if we apply the same argument at higher ν_X. In the fourth column of Figure 8 are tabulated the numerical results when we take $\nu_X=1.4\times10^{18}$Hz.

We have not applied the inhomogeneous jet model presented by Konigl (1981), since some artifacts are invoked in this model; the magnetic field and relativistic electrons are distributed so as to determine fit the whole range of the composite spectrum. However, the analyses of our observations with such models are also awaited.

V. SUMMARY

The results of the present observations are summarized as follows.

(1) Mkn421 was in a relatively faint state in 1984 January and March at frequencies from IR through X-rays.

(2) From January to March, Mkn421 decreased its flux in the IR to X-ray bands. X-ray emission decreased by a factor of 2∿3 while IR-UV radiation decreased by 15∿25 percent. Radio emission remained essentially stable.

(3) The change in the X-ray spectral shape suggests that X-ray emission has two components; the soft component is probably the synchrotron radiation and the hard component was more violently variable and may be ascribed to other mechanisms such as the inverse Compton scattering of synchrotron photons.

(4) The break was observed at a frequency of around 10^{15}Hz; The power law index of IR-optical part is 0.5∿0.8, while for the UV range it is ∿1.0.

(5) At the optical band, the degree of polarization showed a factor 2 variation on the time scales of a few days, while the position angle remained constant during the present observations. The degree of polarization in the IR-optical region shows no wavelength dependence.

(6) The radio spectrum is flat and the extrapolation from the radio spectrum intersects the extrapolation from IR at a frequency of a few times 10^{12}Hz, below which the synchrotron self absorption plays an important role.

(7) Applying the homogeneous synchrotron source theory to the observed results, physical source parameters are deduced. Source size should be less than about 10^{-2}mas. If the source size is less than a few times

10^{-3} mas, relativistic beaming is required. The source is magnetic field dominated and the relativistic electrons with relatively low energy are responsible for the synchrotron radiation. The cooling time of electrons is shorter than the light crossing time, implying that there must be in situ acceleration of the electrons.

(8) The spectral variations in the five week interval are hard to interprete. One possibility is that the source expanded along with an increase of relativistic beaming factor.

Acknowledgements

Some of the optical observations at Okayama were kindly made for this program by Dr.K.Misawa, Y.Fujime and M.Kondo. The IR data at January 30 and February 4 and 6 were kindly provided by Dr.E.I.Robson. We appreciate their cooperation. The work at the University of Michigan was supported by the National Science Foundation under grant No. AST 83-01234.

REFERENCES

Aaronson,M. 1978, Ap.J.(Letters), 221, L103.

Allen,D.A. 1976, Ap.J., 207, 367.

Baath,L.B. 1984, in 'IAU symposium No.110 VLBI and Compact Radio Sources', ed. R.Fanti et al. (Reidel) p.127.

Baath,L.B., Elgered,G., Lundqvist,G., Graham,d., Weiler,K.W.,

Seielstad,G.A., Tallqvist,S., and Schilizzi,R.T. 1981, Astr.Ap., 96, 316.

Bailey,J., Cunningham,E.C., Hough,J.H., and Axon,D.J. 1981, M.N.R.A.S., 197, 627.

Blackwell,D.E., Leggett,S.K., Petford,A.D., Mountain,C.M., and Selby,M.J. 1983, M.N.R.A.S. 205, 897.

Blandford, R.D. 1984, in 'Eleventh Texas Symposium on Relativistic Astrophysics', ed. D.S.Evans (New York Academy of Sciences) p.303.

Bregman,J.N. et al. 1982, Ap.J., 253, 19.

Bregman,J.N. et al. 1984, Ap.J., 276, 454.

Frogel,J.A., Persson,S.E., Aaronson,M., and Matthews,K. 1978, Ap.J. 220, 75.

Frogel,J.A., Persson,S.E., Aaronson,M., Becklin,E.E., Matthews,K., and Neugebauer,G. 1975 Ap.J.(Letters), 200, L123.

Glass,I.S. 1984, M.N.R.A.S., 211, 461.

Glassgold,A.E. et al. 1983, Ap.J., 274, 101.

Gould,R.J. Astr.Ap., 1979, 76, 306.

Hagen-Thorn,V.A., Marchenko,S.G., Smehacheva,R.I., and Yakovleva,V.A. 1983, Astrophyzika, 19, 199.

Hearn,D.R., Marshall,F.J., and Jernigen,J.R. 1979, Ap.J.(Letters), 227, L63.

Hickson,P., Fahlman,G.G., Auman,J.R., Walker,G.A.H., Menon,T.K., and Ninkov,Z. 1982, Ap.J., 258, 53.

Hutter,D.J., and Mufson,S.L. 1985, preprint.

Impey,C.D. 1983, M.N.R.A.S., 202, 397.

Johnson,H.L. 1966, Ap.J., 143, 87..

Joyce,R.R., and Simon,M. 1976, Publ.Astron.Soc.Pac., 88, 870.

Kapahi,V.K. 1979, Astr.Ap., 74, L11.

Kikuchi,S., and Mikami,Y. 1986, in preparation.

Kinman,T.D. 1978, in 'Pittsburgh Conference on BL Lac Objects', ed. Wolfe,M.L., (Pittsburgh University) p.82.

Kondo,Y. et al. 1981, Ap.J., 243, 690.

Konigl,A. 1981, Ap.J., 243, 700.

Koyama,K. et al. 1984, Publ.Astron.Soc.Japan, 36, 659.

Marscher,A.P. 1977, Ap.J., 216, 244.

Marscher,A.P. 1983, Ap.J., 264, 296.

Marscher,A.P., Marshall,F.E., Mushotzky,R.F., Dent,W.A., Balonik,T.J., and Hartman,M.F. 1979, Ap.J., 233, 498.

Margon,B. Jones,T.W., and Wardle,J.F.C. 1978, A.J., 83, 1021.

Maza,J., Martin,P.G., and Angel,J.R.P. 1978, Ap.J., 224, 368.

Mufson,S.L. et al. 1980, Ap.J., 241, 74.

Mufson,S.L. et al, 1984, Ap.J., 285, 571.

Mushotzky,R.F., Boldt,E.A., Holt,S.S., and Serlemitsos,P.J. 1979, Ap.J.(Letters), 232, L17.

O'Dell,S.L., Puschell,J.J., Stein,W.A., Owen,F., Porcas,R.W., Mufson,S., Moffet,T.J., and Ulrich,M.H. 1978a, Ap.J., 224, 22.

O'Dell,S.L., Puschell,J.J., Stein,W.A., and Warner,J.W. 1978b, Ap.J.Suppl, 38, 267.

Persson,S.E., Frogel,J.A., and Aaronson,M. 1979, Ap.J.Suppl., 39, 61.

Riegler,G.R., Agrawal,P.C., and Mushotzky,R.F. 1979, Ap.J.(Letters), 233, L47.

Tanaka,Y. et al. 1984, Publ.Astron.Soc.Japan, 36, 641.

Ulrich,M.H., Kinman,T.D., Lynds,C.R., Rieke,G.H., and Eckers,R.D. 1975, Ap.J., 198, 261.

Ulrich,M.H., Hackney,K.R.H., Hackney,R.H., and Kondo,Y. 1984, Ap.J., 276, 466.

Ulvestad,J.S., Johnston,K.J., and Weiler,K.W. 1983, Ap.J., 266, 18.

Urry,C.M. et al. 1985, preprint.

Warwick,R.S., McHardy,I.M., and Pounds,K.A. 1985, Space Sci.Rev., 40, 597

Wehrle,A.E., Preston,R.A., Meier,D.L., Gorenstein,M.V., Shapiro,I.I., Rogers,A.E.E., and Rius,A. 1984, Ap.J., 284, 18.

Weiler,K.W. and Johnston, K.J. 1980, M.N.R.A.S., 190, 269.

Wills,B.J. et al. 1983, Ap.J., 274, 62.

Worrall,D.M., Boldt,E.A., Holt,S.S., Mushotzky,R.F., and Serlemitsos,P.J. 1981 , Ap.J., 243, 53.

Worrall,D.M. et al. 1982, Ap.J., 261, 403.

Worrall,D.M. et al. 1984a, Ap.J., 278, 521.

Worrall,D.M. et al. 1984b, Ap.J., 284, 512.

Worrall,D.M., Puschell,J.J., Rodrigues-Espinosa,J.M., Bruhweiler,F.C., Miller,H.R., Aller,M.F., and Aller,H.D., 1984c, Ap.J., 286,711.

Table 1

Organization of observations

Observatory	Band	Observers
TENMA	X-Ray	Makino,Tanaka,Matsuoka,Koyama,Inoue,
	1.5-30keV	Makishima,Hoshi,Hayakawa
IUE	UV	Kondo,Urry,Mufson,Hackney,Hackney
	1200-3000Å	
Mt.Lemon	optical	Wisniewski
	U,B,V,R,I	
Okayama	optical	Kikuchi,Mikami
and Dodaira	U,B,V,R	
	with polarimetry	
Agematsu	IR	Hiromoto,Nishida
	J,H,K	
UKIRT	IR	Burnell,Brand,Williams,Smith
	J,H,K,L,L',M,N	
	with J,H,K polarimetry	
NRO	Radio	Takahara,Inoue,Tsuboi,Tabara,Kato
	10,22,43GHz	
Michigan	Radio	Aller,Aller
	4.8,8.0,14.5GHz	

Table 2

Results of UV observations by IUE

Date	Image	$A^{+)}$ (mJy)	$\alpha^{\#)}$	χ^2/DOF	Integrated flux$^{*)}$
Jan.23	LWP2669	6.65±0.12	1.04±0.04	0.71	6.01±0.11
	LWP2700				
	SWP22082				
Jan.28	LWP2711	6.35±0.20	1.01±0.07	0.55	5.82±0.11
	LWP2712				
	SWP22128				
Feb.2	LWP2732	6.77±0.15	1.13±0.20	0.11	5.88±0.18
Mar.3	LWP2881	5.24±0.18	1.10±0.08	1.09	4.61±0.16
	LWP2882				
	SWP22398				
Mar.9	LWP2915	5.04±0.21	1.12±0.08	0.47	4.38±0.14
	SWP22445				

+) the flux density at 3000Å

#) the spectral index for 1200-3000Å

*) integrated over 1200-3000Å and in units of 10^{-11} erg $cm^{-2}s^{-1}$

Table 3

List of telescopes for optical observations

and the aperture correction for the underlying galaxy

Observatory	Diameter (cm)	Aperture (arcsec)	Date	Aperture Correction V magnitude
Okayama	91	37.1	Jan23	13.82
		27.9	Jan29,Mar3,4,6	14.05
	188	8.9	Jan29,31	14.98
		11.8	Jan28	14.72
Dodaira	91	18	Feb7,29	14.39
		13	Feb.6,9,Mar1-12	14.65
Mt.Lemon	100	29.7	Jan24-Feb1,Mar9	14.00
	150	12.4	Mar1-8	14.68

Table 4
Observed optical fluxes and derived fluxes of non-thermal component

Date 1984(UT)	Aperture arcsec	Observed F(U)	F(B)	F(V)	F(R)	F(I)	non-thermal F(U)	F(B)	F(V)	F(R)	F(I)
				mJy					mJy		
					Okayama						
Jan23.80	37.1	8.96	12.25	18.69			7.61	7.51	7.22		
25.74	27.9	8.40	11.70	16.89			7.31	7.86	7.61		
28.80	11.8	7.94	9.91	13.79	19.52		7.36	7.84	8.79	10.60	
29.64	8.9	7.73	9.56	13.05	17.81		7.27	7.93	9.11	10.78	
31.65		8.40	10.38	13.67	17.48		7.93	8.75	9.73	10.46	
Mar 3.53	27.9	7.38	11.07	17.53			6.29	7.23	8.24		
4.82		7.05	10.58	18.02			5.96	6.74	8.73		
6.74		7.31	10.29	16.89			6.23	6.45	7.61		
					Mt.Lemon						
Jan24.43	29.7		11.38	18.02				7.36	8.30		
25.40			11.07	17.53				7.05	7.81		
26.43			11.70	18.52				7.68	8.80		
28.33			10.77	17.85				6.75	8.13		
29.39			11.38	17.37				7.36	7.65		
31.44			11.38	18.02				7.36	8.30		
Feb 1.34			11.70	18.18				7.68	8.46		
Mar 1.35	12.4	7.25	9.73	14.31	20.44	27.64	6.64	7.58	9.12	11.18	12.31
2.26		6.79	9.38	13.42	20.26	27.39	6.18	7.23	8.22	11.00	12.06
3.34		6.67	9.04	13.54	19.52	27.14	6.06	6.89	8.35	10.26	11.81
4.31		6.67	8.88	13.54	19.34	26.64	6.06	6.73	8.35	10.09	11.31
5.36			9.04	14.05				6.89	8.85		
6.30		6.25	8.64	12.58	18.82	25.45	5.64	6.49	7.38	9.56	10.11
7.26		6.73	8.88	13.67	19.70	25.68	6.12	6.73	8.47	10.45	10.35
8.30		6.25	8.56	12.93	18.65	25.92	5.64	6.41	7.74	9.39	10.59
9.29	29.7		9.38	15.27				5.36	5.54		
					Dodaira						
Feb 6.79	13.0	8.27	10.67	15.23	22.08		7.65	8.46	9.89	12.56	
7.83	18.0	9.42	11.95	17.55	25.25		8.63	9.14	10.76	13.15	
9.78	13.0	8.58	10.86	15.91	22.66		7.96	8.65	10.56	13.14	
29.76	18.0	7.72	10.29	15.56	22.43		6.92	7.48	8.77	10.34	
Mar 1.65	13.0	7.29	9.68	14.22	20.46		6.66	7.47	8.87	10.94	
2.60		7.03	9.26	13.62	19.61		6.40	7.05	8.28	10.09	
4.63		6.25	8.40	12.82	18.80		5.62	6.19	7.48	9.28	
5.64		6.36	8.55	12.93	18.80		5.74	6.34	7.59	9.28	
6.71		6.30	8.55	12.93	18.80		5.68	6.34	7.59	9.28	
7.68		6.36	8.55	12.93	18.64		5.74	6.34	7.59	9.13	
8.61		6.66	8.86	13.27	19.12		6.03	6.65	7.93	9.60	
10.68		6.54	8.78	13.39	19.44		5.91	6.57	8.04	9.93	
11.60		6.78	9.02	13.39	19.28		6.15	6.81	8.04	9.76	
12.71		6.48	8.70	12.82	18.64		5.85	6.49	7.48	9.13	

Table 5

The polarization of the non-thermal component

observed in 1984 March 8-12

	U	B	V	R	J	H	K
arcsec	13	13	13	13	7.8	7.8	7.8
%	4.0±0.3	3.3±0.3	3.0±0.2	2.7±0.2	2.5±0.4	2.9±0.3	2.8±0.6
%	4.3±0.3	4.3±0.4	4.7±0.4	5.0±0.4	4.4±0.7	5.0±0.4	4.5±1.0
degree	177±2	175±3	174±2	175±3	179±9	180±5	184±13

In each column the first, second, third and fourth rows show the beam size, the observed degree of polarization, the degree of polarization of the nonthermal component, and the position angle, respectively.

Table 6

Summary of infrared photometric observations

Date	Aperture	J	H	K	L	L'	M	N
(UT)	(arcsec)	240THz 1.25μm 1540Jy	182THz 1.65μm 980Jy	136THz 2.2μm 670Jy	86.9THz 3.45μm 290Jy	78.5THz 3.82μm 250Jy	62.7THz 4.78μm 165Jy	28.6THz 10.5μm 40Jy
Jan25/27	24×60	46.94	57.44	56.24				
Jan30	8	25.56	31.28	33.89	32.69			
Feb4/6	18	38.7	49.1	49.4	40.4			
Mar7/8	24×60	44.83	51.91	54.21				
Mar8	4.8	22.06	26.02	30.62		30.90		
	7.8	26.76	31.86	35.49		31.76		
	11.8	31.88	37.95	41.50				
	6							58±18
Mar9	4.8	23.52	26.74	33.27		35.15		
	7.8	26.27	31.28	34.52		32.65		
	6							58±12
Mar10	7.8	26.03	30.71	32.97		29.8		
	6							36.5±7
Mar11	4.8	22.26	26.26	29.52		30.9	38±6	
	7.8	26.03	31.57	34.20		30.3		
Mar12	4.8	21.65	26.26	25.95		30.0	29±6	
	7.8	26.27	31.86	34.52		35.5		
Jan25/27		17.7	23.9	24.2				
Feb4/6		16.6	22.5	23.4	28.5			
March8/12		15.2	18.1	21.6		27.7	33.2	50.7

The upper panel gives the central frequency, central wavelength and the absolute flux at zero magnitude. The second panel gives the observational results and the third panel shows the fluxes of the non-thermal component in units of mJy. The errors are less than 1 percent unless otherwise indicated.

Table 7

Summary of Radio Observations

(a) NRO 45m

Epoch	10GHz	22GHz	43GHz
Jan.	0.59±0.03	0.47*)	0.49±0.03
March	0.55±0.03	0.55±0.05	0.55±0.1

(b) Univ.Michigan 26m

Epoch	4.8GHz	8.0GHz	14.5GHz
Jan.	0.657±0.034	0.604±0.013	0.540±0.017
March	0.659±0.036	0.62 ±0.03	0.571±0.020

The flux density is shown in units of Jy and the errors are the standard deviation from the mean of daily flux.

*) the data are available only for one day and the error cannot be estimated.

Table 8

The source characteristics deduced from

the synchrotron self Compton model

	January	March		
ν_* (GHz)	2.2×10^{3}	1.5×10^{3}	1.5×10^{3}	1.5×10^{3}
θ_1 (mas)	1.6×10^{-2}	2.3×10^{-2}	2.3×10^{-2}	2.3×10^{-2}
θ_2 (mas)	1.8×10^{-3}	2.7×10^{-3}	2.7×10^{-3}	3.1×10^{-3}
δ	1	1	1.2	1.7
θ_*(mas)	1.8×10^{-3}	2.7×10^{-3}	2.4×10^{-3}	2.2×10^{-3}
t_{1c}(sec)	7.6×10^{4}	1.2×10^{5}	1.0×10^{5}	9.7×10^{4}
γ_a	80	76	80	63
B (G)	1.3×10^{2}	9.5×10^{1}	7.0×10^{1}	7.9×10^{1}
u_{mag}(erg cm^{-3})	6.4×10^{2}	3.6×10^{3}	2.0×10^{2}	2.5×10^{2}
u_{syn}(erg cm^{-3})	1.2×10^{3}	4.0×10^{2}	2.1×10^{2}	5.7×10^{1}
u_{rel}(erg cm^{-3})	3.1	1.2	1.4	3.9×10^{-1}
t_a (sec)	3.3×10^{2}	1.1×10^{3}	1.8×10^{3}	8.5×10^{3}
t_b (sec)	1.6×10^{1}	3.9×10^{1}	8.4×10^{1}	3.9×10^{2}

Figure Captions

Figure 1: The light curves of the nonthermal component of Mkn421. The first panel shows that of the degree of polarization at the V band. The following panels show that of fluxes in the radio (14.5GHz), IR (K band), optical (V band), UV and X-ray frequencies, respectively.

Figure 2: The X-ray spectra obtained by the TENMA satellite. The data were integrated over each observation period.

Figure 3: The IR-optical spectra of Mkn421 in 1984 January-February (Figure 3a) and in March (Figure 3b). The observed fluxes are indicated by filled circles with straight lines: the beam sizes are also shown numerically in the figure. The derived nonthermal fluxes are indicated by open circles.

Figure 4: The composite spectra of of the non-thermal component of Mkn421 in 1984 January and March.

Figure 5: Source parameters obtained by the homogeneous synchrotron theory using the January data. The energy density of magnetic fields u_{mag}, that of synchrotron photons u_{syn}, and the lower limit to the energy density of relativistic electrons u_{rel}^{min} are shown as a function of the angular diameter of the source θ_*mas. The minimum

beaming factor δ_{min} and the Lorentz factor of electrons γ_a which emit the synchrotron radiation at the self absorption turnover frequency are also depicted.

Addresses of Authors

F.Makino, Y.Tanaka, M.Matsuoka, K.Koyama, H.Inoue and K.Makishima

Institute of Space and Astronautical Science

6-1, Komaba 4-chome, Meguro-ku, Tokyo 153, Japan

R.Hoshi

Department of Physics, Rikkyo University

34-1, Nishi-Ikebukuro 3-chome, Toshima-ku, Tokyo 171, Japan

S.Hayakawa

Department of Astrophysics, Nagoya University, Furō-cho

Chikusa-ku, Nagoya 464, Japan

Y.Kondo

Laboratory for Astronomy and Solar Physics, NASA/Goddard

Space Flight Center, Code685, Greenbelt, MD20771

C.M.Urry

Center for Space Research, Massachusetts Institute of

Technology, Cambridge, MA02139

S.L.Mufson

Department of Astronomy, Indiana University

319 Swain West, Bloomington, IN47405

K.R.Hackney, and R.L.Hackney

Department of Physics and Astronomy, Western Kentucky

University, TCCW119, Bowling Green, KY42101

S.Kikuchi, and Y.Mikami,

Tokyo Astronomical Observatory, University of Tokyo

21-1, Osawa 2-chome, Mitaka, Tokyo 181, Japan

W.Z.Wisniewski

Lunar and Planetary Laboratory, University of Arizona

Tuscon, AZ85721

N.Hiromoto

Radio Research Laboratory, 2-1, Nukuikitamachi 4-chome,

Koganei,Tokyo 184, Japan

M.Nishida

Department of Physics, Kyoto University,

Kitashirakawa-Oiwakecho, Sakyo-ku, Kyoto 606, Japan

J.Burnell, and P.Brand

Astronomy Department, University of Edinburgh

Blackford Hill, Edinburgh, EH9 3HJ, Scotland

P.M.Williams, and M.G.Smith

Royal Observatory Edinburgh

Blackford Hill, Edinburgh, EH9 3HJ, Scotland

F.Takahara, and M.Inoue

Nobeyama Radio Observatory, Tokyo Astronomical Observatory

University of Tokyo, Nobeyama, Minamisaku, Nagano 384-13,

Japan

M.Tsuboi

Department of Astronomy, University of Tokyo, 11-16, Yayoi

2-chome, Bunkyo-ku, Tokyo 113, Japan

H.Tabara, and T.Kato

Faculty of Education, Utsunomiya University, 350,

Minemachi, Utsunomiya, Tochigi 321, Japan

M.F.Aller, and H.D.Aller

Department of Astronomy, Dennison Building,

University of Michigan, Ann Arbor, MI48109-1090

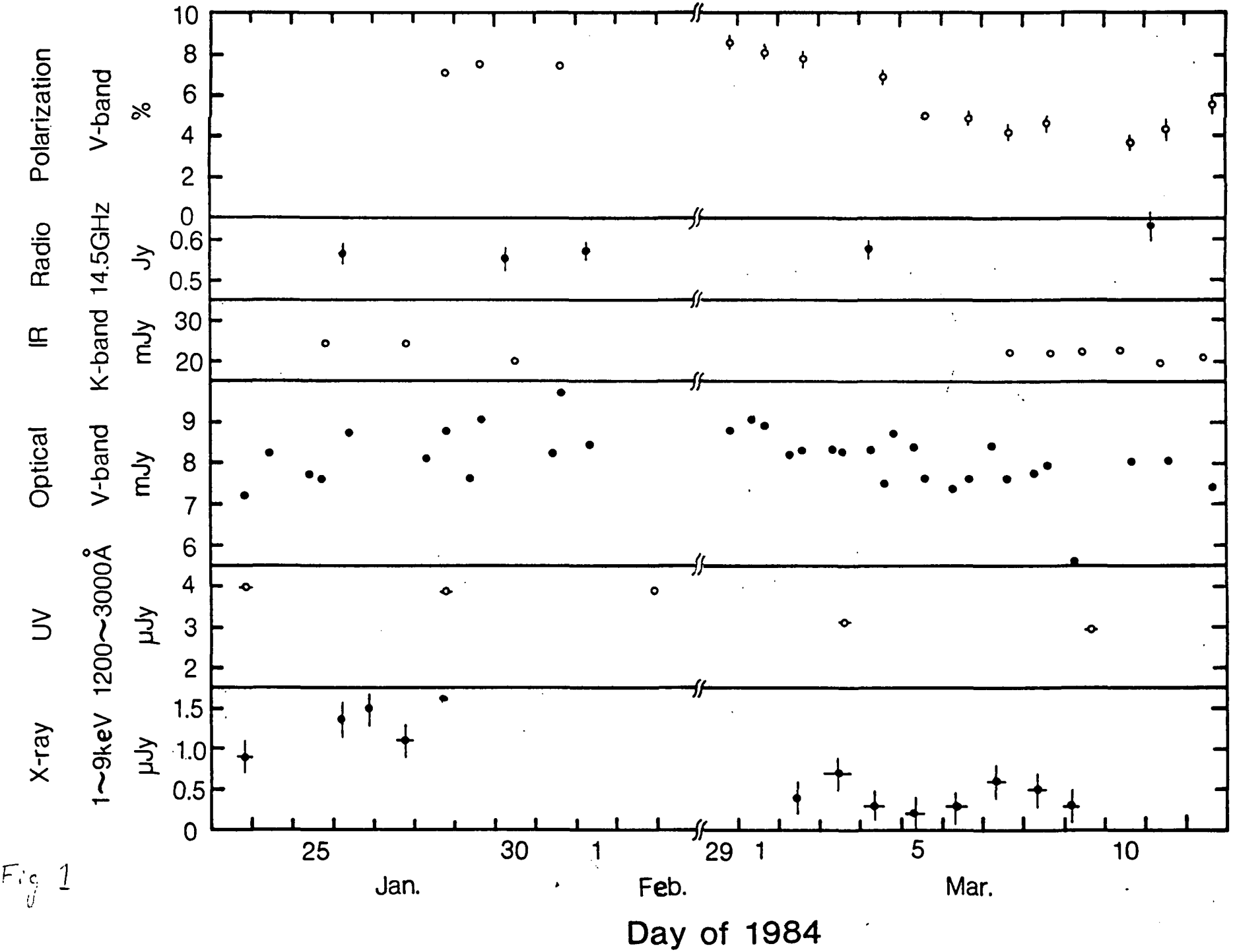
Polarization
V-band
%
10
8
6
4
2
0
Radio
14.5GHz
Jy
0.6
0.5
IR
K-band
mJy
30
20
Optical
V-band
mJy
9
8
7
6
UV
1200~3000Å
μJy
4
3
2
X-ray
1~9keV
μJy
1.5
1.0
0.5
0
25
30
1
29
1
5
10
Jan.
Feb.
Mar.
Day of 1984

Fig 1

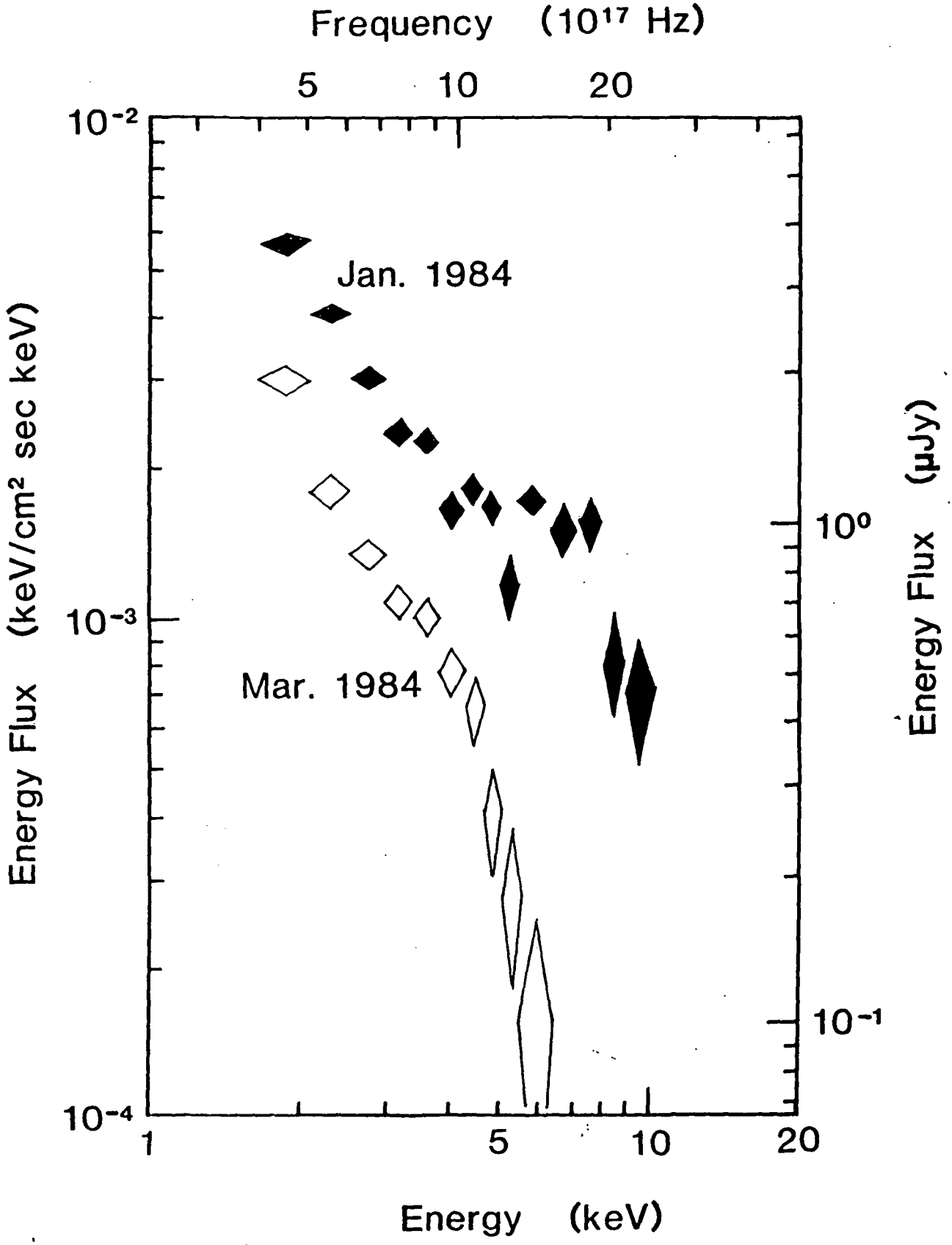
Frequency (10¹⁷ Hz)
5
10
20
10⁻²
10⁻³
10⁻⁴
Jan. 1984
Mar. 1984
Energy Flux (keV/cm² sec keV)
Energy Flux (μJy)
10⁰
10⁻¹
1
5
10
20
Energy (keV)

Fig 3a

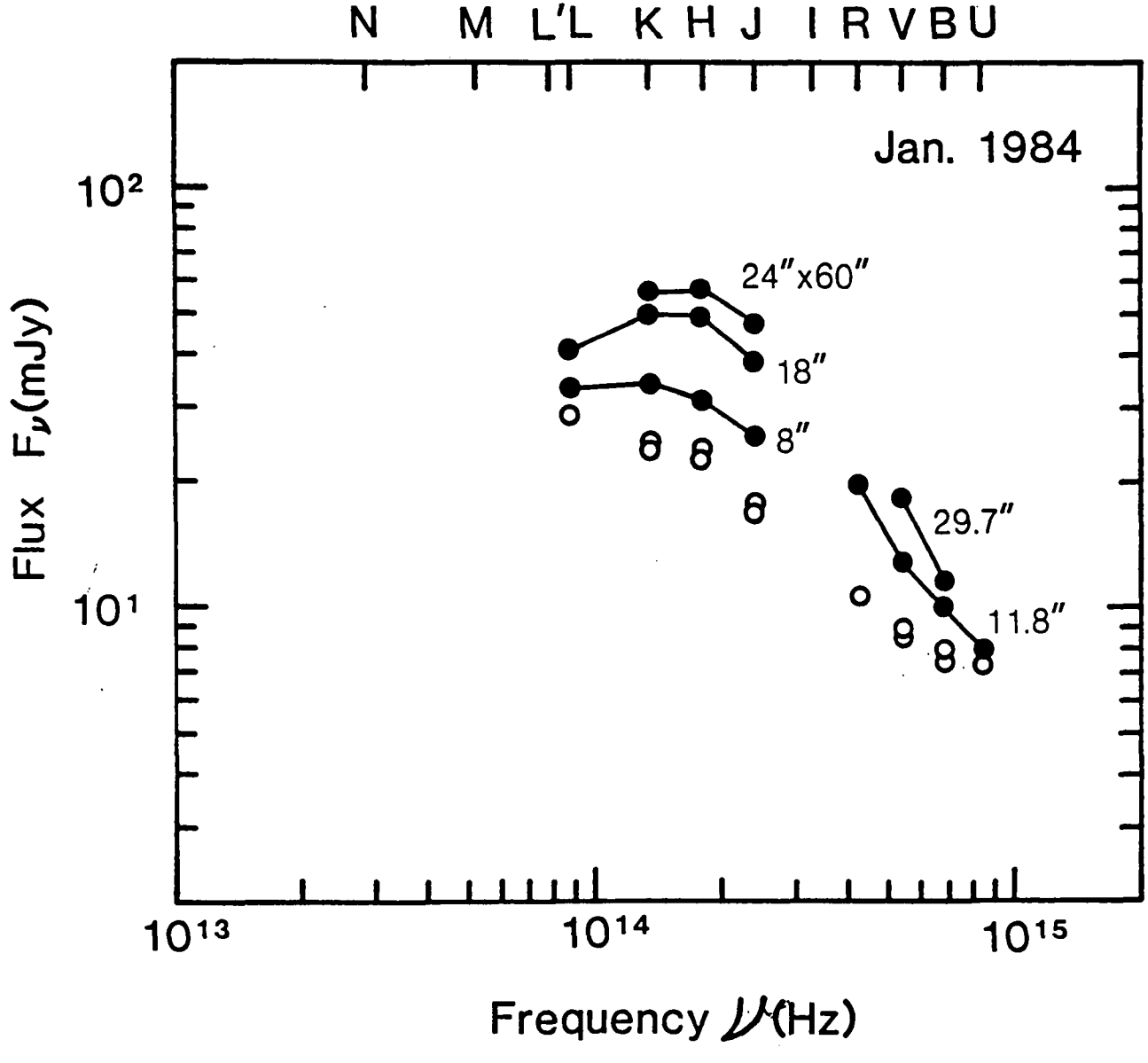
N M L'L K H J I R V B U
Jan. 1984
10^2
10^1
Flux F_ν(mJy)
24"x60"
18"
8"
29.7"
11.8"
10^{13}
10^{14}
10^{15}
Frequency ν(Hz)

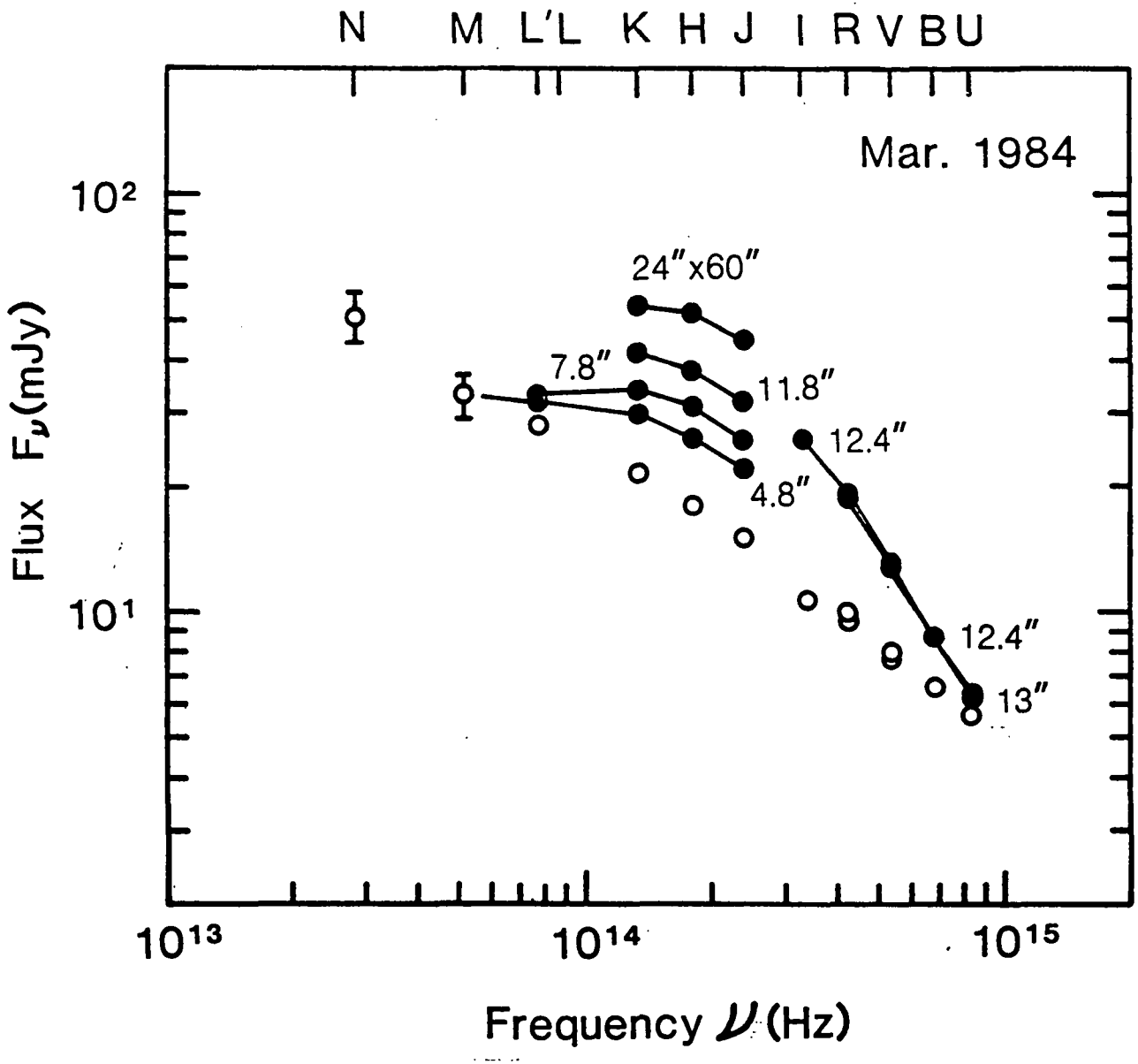
N
M
L'L
K
H
J
I
R
V
B
U
Mar. 1984
10^2
10^1
Flux F_ν(mJy)
24"x60"
7.8"
11.8"
12.4"
4.8"
12.4"
13"
10^{13}
10^{14}
10^{15}
Frequency ν (Hz)

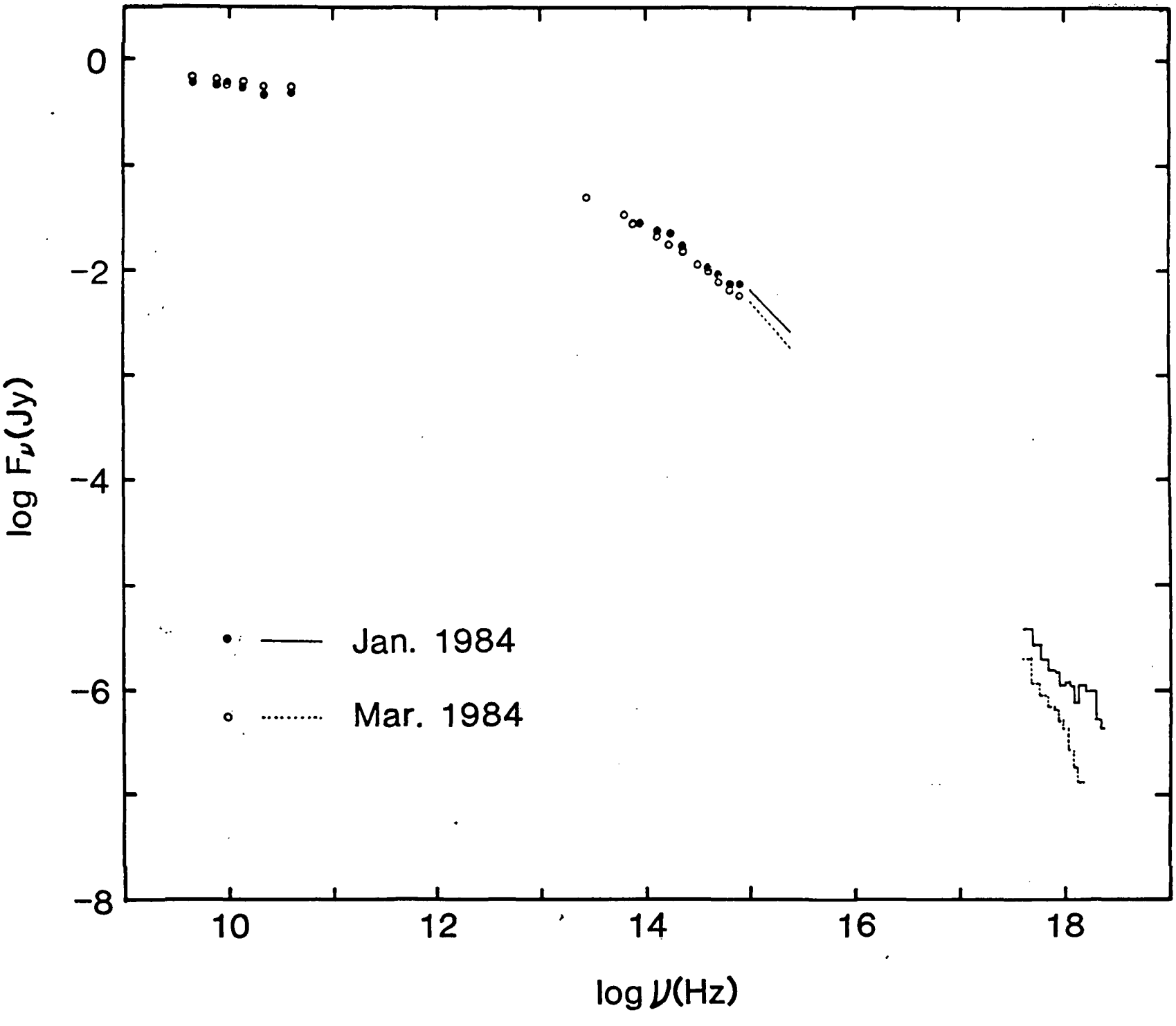
0
−2
−4
−6
−8
10
12
14
16
18
log F_ν(Jy)
log ν(Hz)
Jan. 1984
Mar. 1984

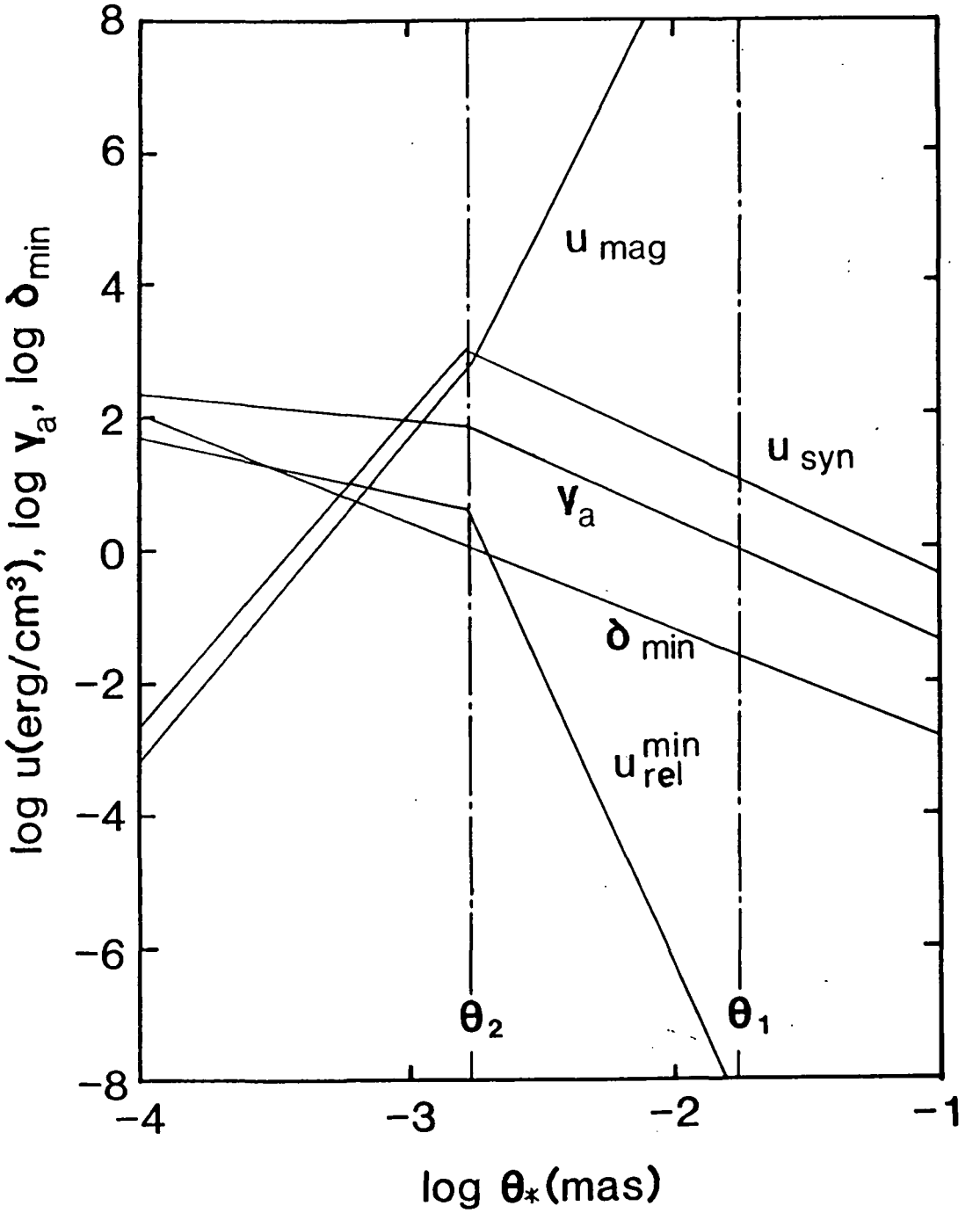
8
6
4
2
0
−2
−4
−6
−8
−4
−3
−2
−1
log u(erg/cm³), log γa, log δmin
log θ*(mas)
u mag
u syn
γa
δ min
u min rel
θ2
θ1